Kinematic Benefits of a Cable-Driven Exosuit for Head-Neck Mobility

Ian Bales and Haohan Zhang, *Member, IEEE*

***Abstract*—This letter presents a novel cable-driven exosuit intended for head-neck support and movement assistance. Mobility limitations in the head-neck, such as dropped head syndrome, can result from various neurological disorders. Current solutions, ranging from static neck collars to rigid-link robotic neck exoskeletons, are unsatisfactory. Neck collars are the most used clinically but fail to restore head-neck motion. Rigid-link neck exoskeletons can enable head movement but are bulky and restrictive. In this letter, we present the design of this exosuit, an analysis of its ability to balance the gravitational moment of the head in simulation, and the results of a user study comparing its kinematic performance to a state-of-the-art rigid-link neck exoskeleton. The exosuit is able to support the head across its full range of motion according to simulation results. It fits users of different sizes and participants exhibited more natural head-neck movement wearing the exosuit as compared to wearing the rigid-link exoskeleton. The exosuit allowed more head rotations than the rigid-link neck exoskeleton and required less compensatory torso movement for three daily tasks (looking for traffic, drinking from a bottle, and picking up an object from the floor). Its absolute range of motion was also much larger than the one allowed by the rigid-link neck exoskeleton. These results demonstrate the kinematic benefits of a cable-driven neck exosuit and provide justification for studying the use of such an exosuit for head-neck movement assistance in patient groups.**

***Index Terms*—Prosthetics and exoskeletons, wearable robotics, tendon/wire mechanism.**

I. Introduction

MOBILITY of the head-neck is imperative for survival and quality of life, as many activities of daily living (ADLs) require large movements of the cervical spine [1], [2], [3], [4]. This includes scanning surroundings to gather sensory information, engaging in conversations, picking up objects, or drinking from a glass or bottle [2], [3], [4], [5], [6]. Many neuromuscular diseases cause impaired head-neck movement, such as dropped head syndrome, which results from diseases like amyotrophic lateral sclerosis (ALS), muscular dystrophy, and cerebral palsy [7], [8], [9], [10], [11], [12]. To support the head against gravity, thereby maintaining a forward gaze and an upright posture, static neck collars are primarily used clinically [7], [12], [13]. However, these static collars are not suitable for extended use, causing pain, reduced range of motion (ROM), and swallowing and breathing difficulties [14], [15]. Notably, they do not assist or restore head-neck movement.

Robotic neck exoskeletons have been developed to restore head-neck mobility in these patient populations as a result [16], [17], [18], [19], [20], [21]. Most existing solutions have extremely limited ROM [19], [20], [21] and support the head via the chin, which would cause swallowing and breathing difficulties [19], [21]. The best performing, state-of-the-art robot uses rigid links to enable 3D rotations of the head and has been shown to help ALS patients regain head-neck control [17], [18]. To reduce the footprint of this robot for maximum ROM, the kinematics of the linkages were designed to couple rotations and translations of the head according to human subject data [22]. However, due to these added kinematic constraints, the movement allowed by this robot does not always align with a given user's natural head-neck movements, leading to discomfort and challenge of fitting. Additionally, even with the attempts to minimize the footprint, the design is still bulky and the allowed ROM is still limited [22].

In contrast, cable-driven exosuit designs do not impose hard kinematic constraints on biological joints, making such designs more comfortable, less restrictive, and align better with natural movements [23], [24]. Combined with the use of Bowden cables, these designs allow heavy actuators to be placed on parts of the body that are more capable of supporting loads, such as at the pelvis, increasing comfort and reducing visual bulkiness [23], [25], [26]. Given the recent success of exosuits for limbs [23], [24], [25], [27], we hypothesize that a cable-driven exosuit design will enable more natural head-neck movement across a large ROM while adequately supporting the head, thus improving comfort as compared to the state-of-the-art neck exoskeleton. Recently, our group has developed a stationary platform to demonstrate the feasibility of using cables to control six degrees-of-freedom (DOF) head-neck motions [28]. While able to apply sufficient forces and moments on the head to assist head-neck movement, the extent to which such a cable-driven neck robot addresses the kinematics limitations in the rigid-link exoskeletons (e.g., limited ROM, constrained movement) remains unknown. Additionally, this predicate device is chair-mounted and thus is not a wearable solution for completing daily

Received 23 July 2024; accepted 2 November 2024. Date of publication 18 November 2024; date of current version 25 November 2024. This article was recommended for publication by Associate Editor Vineet Vashista and Editor Pietro Valdastri upon evaluation of the reviewers' comments. This work was supported in part by National Science Foundation under Grant CBET 2240508 and in part by the National Institutes of Health under Grant R21EB035378. *(Corresponding author: Haohan Zhang.)*

This work involved human subjects or animals in its research. Approval of all ethical and experimental procedures and protocols was granted by the Institutional Review Board at University of Utah under Application No. IRB#00145893.

The authors are with the Department of Mechanical Engineering and Robotics Center, University of Utah, Salt Lake City, UT 84112 USA (e-mail: haohan.zhang@utah.edu).

This letter has supplementary downloadable material available at https://doi.org/10.1109/LRA.2024.3500878, provided by the authors.

Digital Object Identifier 10.1109/LRA.2024.3500878

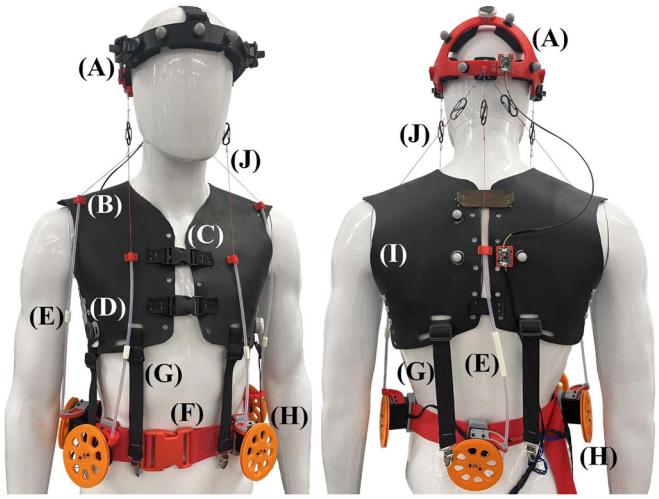

Fig. 1. Front and back view of the exosuit. (A) Headpiece with motion capture markers and IMU. (B) Cable origin point. (C) Front buckle. (D) Side fit dial. (E) Adjustable-length Bowden tubes. (F) Waist belt with buckle. (G) Suspender straps. (H) Servo motors with cable spool. (I) Leather vest with motion capture markers and IMU. (J) Cables with inline carabiners.

tasks that often require full body movements [2], [3], [4]. Our work differs from a previous device that leveraged cables in its design [29]; the motion of that device was governed by the hard kinematics imposed by its rigid linkage, thus having the same limitations as rigid-link neck exoskeletons.

Here, we present the design of a novel cable-driven neck exosuit and its wearability and kinematics performance in healthy subjects. The contributions include the design optimization of the exosuit to support the head across a large ROM and the demonstration of the kinematics improvements of a physical prototype as compared to a state-of-the-art rigid exoskeleton. To the best of our knowledge, this is the first wearable, cable-driven exosuit targeting head-neck mobility and the first in-human study to quantify the kinematic benefits of using an exosuit for head-neck movements.

II. Methods

A. Exosuit Design

A neck exosuit prototype was recently built in the Utah Wearable Robotics Laboratory. This prototype (Fig. 1) consists of braided polyethylene cables routed between a leather vest and a headpiece attached to the trunk and head of the user, respectively. Each cable is actuated by a servo motor via a spool. The motors are mounted on a waist belt, ensuring that the weight of the motors is concentrated on the pelvis. Cable tensions are transmitted through customized Bowden tubes to end stops sewn onto the leather vest that define the *cable origin positions*. Cables are then attached, using carabiners, to three *cable insertion points* on the headpiece; three cables attach to the back point, one cable to the left point, and the final cable to the right point. The carabiners enable quick attachment and release of the cables during donning and doffing and serve as mechanical fuses for safety should any cable tension become too large.

Cable origin and insertion points are chosen based on an optimization that maximizes the transmission ratio between cable tensions and the resultant moment applied on the head using a biomechanical neck model in OpenSim [28], [30]. Using this objective, we were able to identify a design solution where small cable tensions result in a large moment applied on the head. This enables the use of smaller actuators, helping reduce the footprint of the robot while simultaneously maintaining the ability to support the head and assist head-neck movement. To achieve wearability of the exosuit, the cable origin points were constrained to be located on the torso of the user, and the insertion points anywhere on the headband. Initially, a seven cable design was investigated based on our chair-mounted system [28]; however, two front cables on each side coincide in the optimal solution, suggesting that these two cables on each side can be replaced with a single cable for 3D moment control. Therefore, in the physical prototype, we used five cables, which reduces the mechanical complexity compared to our previous chair-mounted system.

The vest can be opened at the front via two buckles. On each side of the vest, under the arm holes, ratcheting dials are available to tighten or loosen the vest, accommodating users of varying sizes. Similarly, the waist belt utilizes a buckle for donning and is adjustable in size. We created PTFE Bowden tubes with spacers for size adjustment. These spacers have a slit on one side to slide over the continuous cable, fitting into and adjusting the length of the Bowden tube for different size users. This avoids using overly long Bowden tubes in order to accommodate all users, reducing friction and improving aesthetics. Adjustable-length suspender straps are available to hold the vest down onto the shoulders of the user. Finally, the headpiece utilizes ratchet connectors to adjust the circumference of the headpiece, as well as a ratcheting dial to adjust the fit of a top strap. The overall shape of the headpiece has been chosen to match the shape of the human head, and $\frac{1}{2}$ in thick foam is placed along its interior to reduce potential pressure points and maximize comfort during use.

B. Kinematics Model, Control, and Simulation

The moment applied on the head is related to the five cable tensions by:

$$\mathbf{m} = A\mathbf{t}, \tag{1}$$

where $\mathbf{m}$ is a 3×1 moment vector, $\mathbf{t} = \begin{bmatrix} t_1 & \cdots & t_5 \end{bmatrix}^{\mathrm{T}}$ is a 5×1 cable tension vector, and A is a 3×5 Jacobian matrix that depends on the position of the cables:

$$A = \begin{bmatrix} \mathbf{b}_1 \times \hat{\mathbf{c}_1} & \cdots & \mathbf{b}_5 \times \hat{\mathbf{c}_5} \end{bmatrix}, \tag{2}$$

where $\mathbf{b}_i$ is the position vector from the base of the neck to each cable's insertion point and $\hat{\mathbf{c}_i}$ is the unit vector pointing from each cable's insertion point to its origin point at a given configuration of the exosuit.

Given a moment $\mathbf{m}$, there exists no analytical solution to determine $\mathbf{t}$ as A is not a square matrix and thus is not invertible. A pseudoinverse strategy is insufficient as there must be lower and upper bounds on cable tensions [31]. To properly distribute

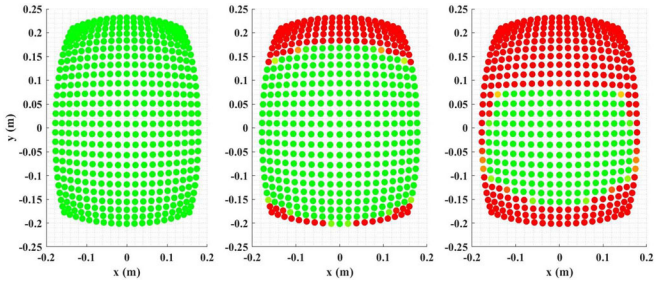

Fig. 2. Simulated moment feasible workspace results at 0° twist angle. View shown is a top-down view of human head workspace. Green dots indicate head positions where gravity compensation is feasible, red otherwise. Left) No upper bound on cable tensions; $\omega = 0$. Center) $t_{\max} = 100$ N; $\omega =$ 1e-5. Right) $t_{\max} = 40$ N; $\omega =$ 1e-5.

the tensions in each cable to apply a desired moment $\mathbf{m}_{des}$ on the head, we devised the following optimization problem:

$$\arg\min_{\mathbf{t}} f(\mathbf{t}) = (\mathbf{m}_{des} - A\mathbf{t})^{\mathrm{T}} (\mathbf{m}_{des} - A\mathbf{t}) + \omega \mathbf{t}^{\mathrm{T}}\mathbf{t}, \quad (3)$$

which seeks to minimize the absolute difference between the desired and actual wrench applied by the robot as well as minimize overall cable tensions, subject to cable tension minimum ($t_{\min}$) and maximum ($t_{\max}$) constraints. ω is a weight parameter that determines the extent to which the optimization algorithm prioritizes reducing the tension vector magnitude over maximizing moment production accuracy, improving efficiency and minimizing the resultant compression force on the cervical spine of the user as a safety measure. This objective function has the gradient:

$$\nabla \mathbf{f}_{5\times 1} = -2A^{\mathrm{T}} (\mathbf{m}_{des} - A\mathbf{t}) + 2\omega\mathbf{t}, \quad (4)$$

which can be used in a gradient descent algorithm to solve for the optimal cable tension $\mathbf{t}$.

This control scheme was implemented in a simulated model of the exosuit in MATLAB (R2023a, MathWorks, MA, USA) to evaluate its moment feasible workspace (MFW), defined as the percentage of the natural workspace of the head in which the exosuit is able to support the head against gravity. Using an inverted pendulum model of the head-neck with a length of 0.17 m and a 4.6 kg head mass [32], the head is positioned through the head-neck's entire natural ROM [33] in 2.5° increments. The moment applied on the head due to the force of gravity $\mathbf{m}_g$ is then calculated. Cable positions are calculated at each head pose, and cable tensions are calculated per (3) where $\mathbf{m}_{des} = -\mathbf{m}_g$. If the calculated moment applied on the head by the cables is within 25% of $\mathbf{m}_g$, then the head is considered supported. This 25% figure accounts for one standard deviation in head mass [32]. This metric is used to evaluate performance as supporting the head against gravity is a critical function of these neck devices, with moments necessary to restore movement to the head being relatively small in comparison to $\mathbf{m}_g$.

Illustrative results are shown in Fig. 2; for visualization purposes, the twist angle was held at 0°. Complete results are shown in Table I, where the head was rotated about all three axes (flexion-extension, bending, and twist). $t_{\min} = 1$ N and $t_{\max} = 40$ N were chosen based on a 4cm spool radius

TABLE I
MOMENT FEASIBLE WORKSPACE RESULTS

$t_{\min}(N)$	$t_{\max}(N)$	ω	MFW (%)
0	∞	0	100
1	100	1e-5	68
		1e-3	43
	40	1e-5	31
		1e-3	26
2	100	1e-5	66
		1e-3	38
	40	1e-5	29
		1e-3	23

combined with the performance characteristics of the Dynamixel XM430-W210-R servo motors (ROBOTIS, Seoul, South Korea). $t_{\min} = 2$ N and $t_{\max} = 100$ N is similarly feasible; however, pilot testing found user discomfort at cable tensions above 40 N using the present exosuit prototype. Without an upper bound on cable tensions and $\omega = 0$, the exosuit is able to support the head through its entire ROM. Limiting $t_{\max}$ or increasing ω decreases the MFW. Generally, a greater $t_{\max}$ and a smaller $t_{\min}$ are advantageous and ω must be chosen carefully to balance performance and comfort.

C. User Study

We performed a user study in healthy adults to demonstrate the kinematic benefits of the exosuit design as compared to a state-of-the-art rigid-link neck exoskeleton. Specifically, we hypothesized that the exosuit would allow for more natural head movements, permit greater head-neck and upper limb ROM, and enable participants to complete daily tasks with more natural head and torso movements than the Utah Exo. The study was approved by the Institutional Review Board (IRB #00145893) at the University of Utah. Participants (5 male, 5 female, mean age: 24.9 yrs, SD: 2.2 yrs) varied in height from 163–188 cm (mean: 174.9 cm, SD: 9.4 cm).

A crossover experiment design was used. Participants were asked to perform tests under three conditions: 1) a baseline with no robot assistance; 2) wearing a rigid-link neck exoskeleton; and 3) wearing the cable-driven neck exosuit. The baseline was always measured first, followed by the Utah Exo and the exosuit in a randomized order. Half of the participants wore the Utah Exo first; the other half wore the exosuit first.

For the baseline condition, the headpiece was mounted on the head of the participant, and the exosuit vest was worn. The headpiece and vest were left disconnected to allow participants to perform natural head movement without any forces or moments applied by the robot. During the exosuit condition, the cables were connected from the vest to the headpiece. The exosuit was then programmed to be in a minimum tension mode where each cable applied a constant 1N tension to prevent cable slacking. During this condition, cable length data were also collected.

For the rigid-link exoskeleton condition, a replica of a state-of-the-art neck exoskeleton (Utah Exo [34]) was used. The Utah Exo enables three DOF head-neck movement (coupled rotation and translation) [34]. During use, it is fixed on the user at the

forehead and the shoulders through a headband and a shoulder attachment, respectively. Three servo motors are mounted on the shoulder attachment; each actuates a linkage chain that connects the shoulder attachment with the headband. Hence, the head motions of the user are determined by the exoskeleton kinematics, which is a fundamental difference from the exosuit. In the current experiment, the Utah Exo was properly fitted on the shoulders of the participant and tightened using underarm straps. Because the headpiece of the exosuit was designed to be compatible with the Utah Exo's kinematics, the same headpiece was used for all conditions, thus eliminating head attachment method from affecting the outcomes. When using the Utah Exo, the motor torques were turned off. The Utah Exo is very back-drivable and nearly transparent to the wearer when unpowered [35].

For each condition, four tests were conducted: 1) target reaching; 2) absolute head ROM; 3) upper limb ROM; and 4) simulated activities of daily living (ADLs). A 12-camera motion capture system (Vero, Vicon, Oxford, U.K.) was used to measure head and torso kinematics data through markers placed on the headpiece and the vest. Markers were also placed on an armband worn on the right arm to measure upper limb ROM. Marker trajectories were used to compute rotations following the body-XYZ Euler angles convention.

The target reaching test was designed to quantify each device's ability to facilitate natural head trajectories during use. To evaluate this, four tasks were used. In each task, the participant looked back and forth at a pair of visual targets taped on a wall (Fig. 3) at a speed that they were comfortable with. The participant was instructed to make the best effort to point their nose at each target, ensuring head rotation rather than solely eye movement. One pair of targets was placed at $\pm 30^\circ$ about the twist axis (vertical axis) from the center of the participant's field of view, two other pairs of targets were placed at $\pm 30^\circ$ about the twist axis and $\pm 10^\circ/\mp 10^\circ$ about the flexion-extension axis (horizontal axis), and the last pair was placed at $\pm 10^\circ$ about the flexion-extension axis. For each task, the participant repeated the motion five times continuously.

To assess the absolute head ROM permitted by either device, each participant was asked to rotate their head to its minimum and maximum extent about each axis (flexion-extension, lateral bending, and twisting) three times while the motion capture system measured their head angles. Upper limb ROM was measured by asking the participant to raise their arm as high as possible without being limited by the worn device. For the exosuit, this was the arm angle just before any Bowden tube was dislodged from its end stop. For the Utah Exo, this was the arm angle just before the device lifted off the participant's shoulders or head. At this angle, motion capture recorded the upper limb angle. This was done in both humeral abduction and in humeral flexion [36].

Three ADL tasks were chosen to evaluate the performance of the exosuit design for real-world tasks [2], [3], [4]. These tasks were chosen because they involve relatively large neck movements while also being simple to set up in the motion capture workspace. First, participants completed an object pickup task. This task starts in a standing position, where the participant drops a towel straight out in front of them. They then pick up the towel in their preferred manner (e.g., squat down or without knee bend) before standing back up and repeating the task. Next, the participant completed a water drinking task where they were instructed to attempt to get the final drop out of an empty water bottle. The critical DOF for these two tasks was flexion-extension. Finally, participants completed a traffic check task. Participants were asked to bend slightly forward from the waist and look at a target on a wall to their left, then another target to their right, then stand back up. This simulates looking for traffic before crossing a street. The critical DOF for this task was twist. Each task was repeated five times continuously.

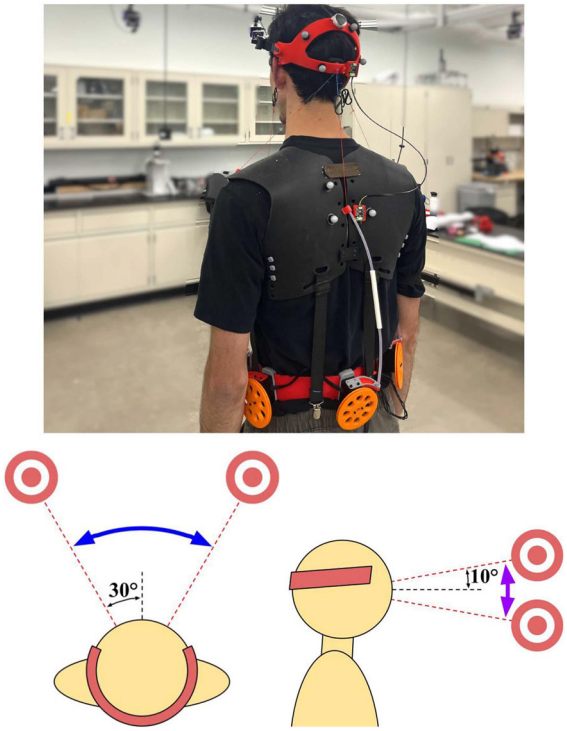

Fig. 3. Target reaching test overview. Top) Participant during target reaching test wearing exosuit. Bottom Left) Twisting task schematic. Bottom Right) Flexion-extension task schematic. Two more tasks were conducted which combined these two movements.

D. Data Processing and Statistical Analysis

Head translation and rotation data for each participant captured during the target reaching test were segmented and time-normalized. The mean trajectory was computed for each condition. To avoid device ROM affecting the results, target reaching task data outside of the ROM allowed by the Utah Exo were discarded (Table II), as the Utah Exo is the most limiting for all DOF. Finally, the *mean trajectory error* was computed for each device as the mean absolute difference between the mean trajectory while wearing each device and the mean trajectory of the baseline trial. This was calculated for each translational and rotational DOF. The position of the proximal posterior marker (Fig. 1) was used for head translation data.

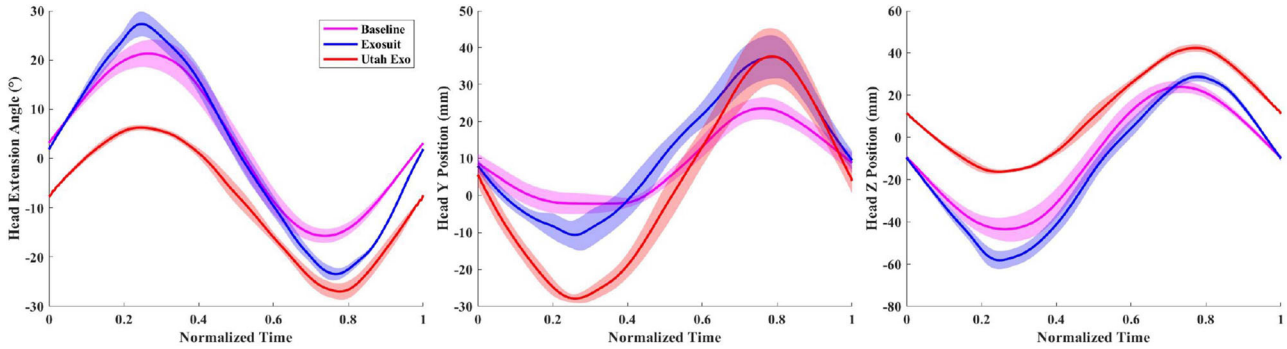

Fig. 4. Representative target reaching test results from one participant during the extension task. Left) Head extension angle vs. normalized time. Center) Head Y position (forward/backward) vs. time. Right) Head Z position (up/down) vs. time. Solid lines represent mean trajectory. Shaded regions indicate ± 1 standard deviation from the mean.

TABLE II
ABSOLUTE ROM RESULTS

DOF	Condition	Min. Angle (°) Mean (StdDev)	Max. Angle (°) Mean (StdDev)
		$*$ ⇔ Significant Results	
Head Extension	Baseline	-72 (6.1)	62 (9.8)
	Exosuit	-62* (5.8)	57* (8.1)
	Utah Exo	-56 (15)	20* (11)
Head Bending	Baseline	-46 (6.2)	46 (5.9)
	Exosuit	-43 (6.7)	43 (7.3)
	Utah Exo	-17* (5.9)	14* (5.0)
Head Twist	Baseline	-77 (7.5)	77 (5.3)
	Exosuit	-66* (7.3)	67* (8.2)
	Utah Exo	-32* (13)	21* (10)
Humeral Abduction	Baseline		129 (15)
	Exosuit		126 (20)
	Utah Exo		85* (21)
Humeral Flexion	Baseline		124 (14)
	Exosuit		125 (9.7)
	Utah Exo		92* (14)

Head ROM was computed as the largest positive and negative angle reached during the ROM assessment task about each rotational axis. *Upper limb ROM* was computed as the mean angle recorded during the upper limb ROM test for humeral abduction and flexion. *ADL ROM* was computed first by segmenting head and torso rotation data during each ADL task and computing the mean trajectory for the critical DOF. Then, the maximum angle of the mean trajectory was recorded for both head and torso.

All kinematics data were measured relative to a neutral position for each condition. Friedman's tests were conducted first to compare outcome variables (*mean trajectory error*, *head ROM*, *upper limb ROM*, and *ADL ROM*) across conditions (baseline, exosuit, Utah Exo), with consideration of secondary factors such as sex (male, female) and height (short: < 175 cm, tall: ≥ 175 cm). Pairwise statistical comparisons were then made for each outcome variable between the exosuit and the Utah Exo, as well as between the exosuit and baseline condition where applicable. Results between sex and height categories were also compared. Wilcoxon signed-rank tests were utilized as the data are not necessarily normally distributed. The statistical significance level was set at $\alpha = 0.05$. These analyses were performed in MATLAB. Post-hoc power analyses were performed using G*Power (3.1.9.7, University of Düsseldorf, Düsseldorf, Germany) to determine statistical power.

III. RESULTS

Representative data from one participant during one task of the target reaching test (head flexion-extension) are shown in Fig. 4. The trajectories of the exosuit (blue) are close to those of the baseline (magenta). Head trajectories while wearing the Utah Exo (red) appear less similar. Qualitatively, this suggests that the head motion while wearing the Utah Exo may be less natural than while wearing the exosuit because the baseline trajectories were altered more noticeably by the Utah Exo.

Mean trajectory error results are shown in Fig. 5. There is a significant ($p = 0.002$) decrease in twist angle error from the Utah Exo to the exosuit. There is also a significant decrease in X ($p = 0.002$) and Y ($p = 0.024$) translational error from the Utah Exo to the exosuit. These results suggest that the cable-driven exosuit permits more natural head-neck movement than the rigid-link Utah Exo. These results are not affected by participants' sex or height ($p \geq 0.104$).

Results for *head ROM* and *upper limb ROM* are shown in Table II. There is a significant difference between conditions ($p < 0.001$). Across all head rotational DOF, there is an increase in ROM of 147% from the Utah Exo to the exosuit. Except for minimum extension angle (i.e., maximum flexion angle), these increases are significant ($p < 0.001$). For all head rotation angles except for minimum and maximum bending angles, there are significant ($p \leq 0.024$) decreases in ROM from the baseline condition to the exosuit. There is a significant ($p \leq 0.002$) increase in upper limb ROM, in both humeral abduction and flexion, from the Utah Exo to the exosuit. These results are not significantly affected by participant sex or height ($p \geq 0.062$).

ADL ROM results are shown in Table III. Differences between conditions were significant across all tasks ($p \leq 0.018$), independent of participant sex or height ($p \geq 0.366$). There is a significant ($p < 0.001$) increase in head extension angle from the Utah Exo to the exosuit during the drinking task. During the traffic check task, there is a significant ($p < 0.001$) increase in head twist angle and a significant ($p < 0.001$) decrease in torso twist angle from the Utah Exo to the exosuit. The exosuit yields a

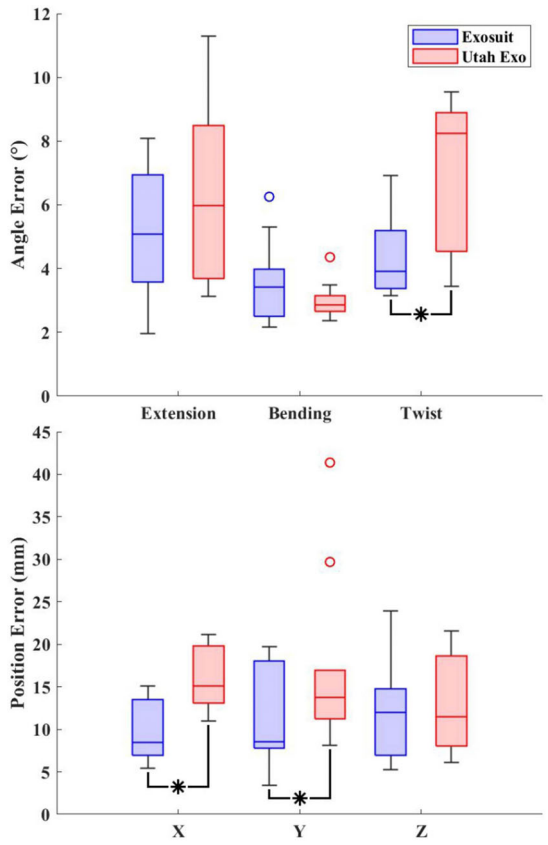

Fig. 5. Mean trajectory errors during entire target reaching test for all participants. Top) Angle error. Bottom) Position error. An asterisk (*) indicates a significant difference between devices.

significant ($p = 0.032$) reduction in head twist angle compared to the baseline. Both devices yield a significant ($p \leq 0.003$) decrease in head flexion angle during the pickup task compared to the baseline.

IV. Discussion

We performed multiple design iterations for the physical implementation of the current prototype according to the following key aspects: 1) accommodation of a wide range of user sizes; 2) a snug fit on the human body to ensure consistent performance; and 3) maximizing user comfort. To accommodate a wide range of user sizes, multiple size-adjustable features were successfully implemented on the exosuit, and no study participant was unable to be accommodated. The choice of leather as the material for the exosuit vest resulted in a suit soft enough to adapt to individual participants' body shapes while maintaining adequate structural stiffness to stay snugly attached when subjected to cable tensions. The exosuit fit snugly on all participants throughout their experiment. Due to the large change of the cable directions at the shoulder cable origin point, lifting of the exosuit off of the user's body was observed during pilot testing. To address this, the ratcheting dials and suspender straps were added, which reduce the lift-off of the vest from the user's body, potentially improving overall performance. Analysis of the effectiveness of these solutions to maintain consistent robot performance will be necessary in future studies in which the exosuit provides movement assistance. All study participants reported acceptable comfort of the exosuit.

TABLE III
ADL Functional ROM Results

Task	DOF	Condition	Max. Angle (°) Mean (StdDev) ∗ ⇔ Significant Results
Pickup	Head Flexion	Baseline	26 (7.2)
		Exosuit	16* (6.5)
		Utah Exo	11* (8.7)
	Torso Flexion	Baseline	60 (10)
		Exosuit	61 (19)
		Utah Exo	56 (20)
Drink	Head Extension	Baseline	52 (18)
		Exosuit	51 (14)
		Utah Exo	20* (8.2)
	Torso Extension	Baseline	9.6 (6.6)
		Exosuit	11 (6.2)
		Utah Exo	15 (10)
Traffic Check	Head Twist	Baseline	30 (11)
		Exosuit	22* (10)
		Utah Exo	3.6* (4.5)
	Torso Twist	Baseline	7.1 (4.6)
		Exosuit	8.0 (4.7)
		Utah Exo	18* (9.4)

Potential design limitations were identified. The limits of the exosuit's size adjustments were reached during our study; users under 163 cm or over 188 cm tall would be better served with a smaller or larger version of the exosuit, respectively. The increase from three servo motors in the exoskeleton to five of the exosuit results in a slight increase in mass of the system, from 1.2 kg for the Utah Exo to 1.5 kg for the exosuit. To compensate for this, the motors were placed on a waist belt, and participants did not report any discomfort from this increase in system weight. The headpiece may cause discomfort as it clamps down on the front and back of the user's head. Our design was effective at limiting this potential issue, as no participant reported headaches or head discomfort. However, participants' forehead skin was reddened where it was in contact with the headpiece. Increasing the surface area of this part of the headpiece would reduce the pressure at the same clamping force, potentially mitigating this issue. In minimum tension mode, cable slacking may occur as the commanded torque is too low to overcome the motor dynamics. In real-world use, motor torques will be greater, preventing slacking. Should slacking still occur, a cover has been designed for the cable spools to prevent unspooling.

Target reaching test results suggest that the exosuit enables more natural head-neck movement than the Utah Exo, as the exosuit enabled trajectories that were more similar to the baseline trajectories than the Utah Exo did. Analysis was done carefully to avoid the influence of the Utah Exo's limited ROM since our aim was to evaluate the impact the device had on natural movements within its ROM rather than testing the impact of its absolute ROM restriction. For example, the Utah Exo was unable to facilitate head twisting past 16° on average; this would have resulted in high twist trajectory errors as the participant was

asked to try to rotate their head up to 30°. Discarding data points above the ROM limits of the most restrictive device (the Utah Exo, in all cases) ensured that the results accurately represented the ability of the devices to allow for natural head trajectories in all six DOF. All participants responded that they felt the exosuit enabled more natural head-neck motions than the Utah Exo. However, many felt that improvements could still be made. This is supported by the nonzero observed rotational and translational error for the exosuit. Utilizing motors with less friction would enable a lower minimum tension value, decreasing the net force and moment applied to the head of the user during use, likely resulting in more natural head-neck movements when wearing the exosuit.

Compared to the Utah Exo, the exosuit had a significant increase in absolute ROM for all except the head flexion angle. The Utah Exo ROM in this study was similar to published bench results [34], with small discrepancies in maximum bending and twisting angle in healthy users. This suggests that while the Utah Exo can achieve its designed ROM, its rigid kinematics make it difficult to fit users of different sizes and with different motion characteristics. In contrast, the exosuit allowed much higher ROM consistently across all participants due to its softness by design. However, the exosuit ROM in all DOF (except head bending) was still significantly less than the baseline. This could be caused by the fact that the net torque, produced by the minimal tension in all cables, was noticeable by the participants, causing them to alter their movement behavior. Again, utilizing motors with less friction may address this limitation.

While absolute head-neck ROM is important, the full range of head-neck motion may not be required during daily tasks. Compared to the Utah Exo, the exosuit permitted more head movement and required less compensatory torso movement during each ADL task. Compared to the baseline, the exosuit reduced head motion during the pickup and traffic check tasks but did not require more torso movement. The Utah Exo reduced the users' ability to extend their heads to drink from a bottle. The most significant results were during the traffic check task. With the Utah Exo, participants kept their heads nearly still relative to the torso and instead twisted their torso to complete the task. This demonstrates the benefits of the exosuit compared to the rigid-link neck exoskeleton in a real-world scenario because users can move their heads more for daily tasks without needing compensatory torso movements to complete these tasks.

Devices' physical design affects upper limb ROM. The Utah Exo utilizes a rigid surface for the motors to attach to, which sits on top of the users' shoulders. This rigid interface inhibits ROM by interfering with raising the arm above shoulder level. Additionally, the rigid-link structure passes movement of the shoulder attachment to the headpiece of the device; lifting an arm above shoulder level can then result in the headpiece moving up and off the head of the user. This was reflected in the upper limb ROM results, as both directions of movement were limited to approximately 90°. The exosuit is able to use a softer interface between device and user, permitting unrestricted upper limb movement according to the data. Note that if the Bowden tubes were too short, lifting the arm could pop the Bowden tubes out of their end stops. This was mitigated through the use of the spacers to adjust Bowden tube lengths.

The study presented in this letter has potential limitations. Healthy participants do not necessarily represent the behavior of individuals with mobility limitations; however, testing with healthy participants first was necessary to validate safety and comfort, explore and compare the physical limits of these devices, and identify any design flaws. There is little diversity in participants' age. Increasing diversity in age and physical condition is necessary for future studies. Increasing sample size would yield greater confidence in the stated claims; however, a post hoc power analysis revealed that the study was adequately powered for the reported significant results (e.g., the absolute ROM increase in maximum twist angle from the Utah Exo to the exosuit ($n = 10$) has a power > 0.99). As this was a short-term feasibility study, long-term outcomes such as potential adverse effects of the exosuit were not measured. Future long-term studies will be conducted to address this.

Direct comparisons were made only to the Utah Exo for multiple reasons. Obtaining access to all other existing research devices is infeasible and unnecessary. Some of these devices do not restore three DOF head mobility and thus are inadequate for restoring healthy head-neck motion entirely. The Utah Exo also exhibits a larger ROM than the other devices. This leaves the Utah Exo as the current leading solution for assisting head-neck motion and therefore the best candidate for direct comparison to the exosuit.

Simulation results show that this exosuit design is able to support the head across a large portion of the natural ROM of the head, subject to limitations based on motor performance constraints. As a result, it is important to select servo motors with a wide torque band; motors able to operate at both a smaller minimum torque and greater maximum torque will yield a larger MFW. Additionally, ω must be small enough to permit a satisfactory MFW while large enough to keep overall cable tensions low and maximize user comfort. Even in the worst-case scenario presented in Table I, the exosuit can support the head in a region centered around the neutral upright position. In the best case, the exosuit is able to support the head across its entire ROM. However, simulation results alone do not account for the complexities of real-world use. To overcome this limitation, real-world testing will be conducted as part of future investigations.

Another future improvement is the real-time measurement of head pose since control of the exosuit requires real-time cable position information to compute the Jacobian matrix A. With only five cables in the current prototype, an analytical solution to compute the position of each cable insertion point using cable length data (i.e., forward kinematics) does not exist. IMUs were considered as a solution to measure the orientation of the head; however, the IMUs used in the current model are not accurate enough for consistent measurement. To overcome this, cable length data were collected through the motor encoders during the study presented in this letter. Along with the position and orientation data of the head measured by the motion capture cameras, these data can potentially be used to create a data-driven forward kinematics model to predict cable insertion positions based on cable length. We have previously shown the feasibility of this approach for rigid-link neck exoskeletons [37]. This will enable head-neck motion control for the exosuit for future studies on

the efficacy of the exosuit for supporting the head and assisting head-neck movement in patient populations.

V. Conclusion

In this letter, we presented the design of a wearable cable-driven exosuit for head-neck movement assistance, a simulated analysis of the ability of the exosuit to support the head against gravity, and results from a user study comparing the kinematics benefits of the exosuit against a state-of-the-art rigid neck exoskeleton. The exosuit exhibits a comfortable design that is able to fit users of a wide range of sizes. Simulation results indicate that it can support the head at various head poses covering a considerable amount of the head's natural ROM. The exosuit allowed for more natural head-neck movement and a larger range of motion of the head without limiting the users' upper limb range of motion, as compared to the rigid-linkage neck exoskeleton, including during functional tasks.

Acknowledgment

The authors would like to thank the 10 participants for completing this study.

References

[1] B. Jung, A. C. Black, and B. S. Bhutta, "Anatomy, head and neck, neck movements," in *Statpearls [Internet]*. Tampa FL, USA: StatPearls Publishing LLC, 2023.

[2] D. G. Cobian, N. S. Daehn, P. A. Anderson, and B. C. Heiderscheit, "Active cervical and lumbar range of motion during performance of activities of daily living in healthy young adults," *Spine*, vol. 38, no. 20, pp. 1754–1763, 2013.

[3] C. P. Miller, J. E. Bible, K. A. Jegede, P. G. Whang, and J. N. Grauer, "Soft and rigid collars provide similar restriction in cervical range of motion during fifteen activities of daily living," *Spine*, vol. 35, no. 13, pp. 1271–1278, 2010.

[4] S. E. Bennett, R. J. Schenk, and E. D. Simmons, "Active range of motion utilized in the cervical spine to perform daily functional tasks," *Clin. Spine Surg.*, vol. 15, no. 4, pp. 307–311, 2002.

[5] N. C. Higgins, D. A. Pupo, E. J. Ozmeral, and D. A. Eddins, "Head movement and its relation to hearing," *Front. Psychol.*, vol. 14, 2023, Art. no. 1183303.

[6] L. Groenesteijn, R. P. Ellegast, K. Keller, F. Krause, H. Berger, and M. P. de Looze, "Office task effects on comfort and body dynamics in five dynamic office chairs," *Appl. Ergonom.*, vol. 43, no. 2, pp. 320–328, 2012.

[7] M. Gourie-Devi, A. Nalini, and S. Sandhya, "Early or late appearance of "dropped head syndrome" in amyotrophic lateral sclerosis," *J. Neurol., Neurosurgery Psychiatry*, vol. 74, no. 5, pp. 683–686, 2003.

[8] R. A. Smith and F. H. Norris, "Symptomatic care of patients with amyotrophic lateral sclerosis," *Jama*, vol. 234, no. 7, pp. 715–717, 1975.

[9] S. Bozgeyik, İ. Alemdaroğlu, N. Bulut, Ö. Yilmaz, and A. Karaduman, "Neck flexor muscle strength and its relation with functional performance in duchenne muscular dystrophy," *Eur. J. Paediatric Neurol.*, vol. 21, no. 3, pp. 494–499, 2017.

[10] A. Agarwal and I. Verma, "Cerebral palsy in children: An overview," *J. Clin. Orthopaedics Trauma*, vol. 3, no. 2, pp. 77–81, 2012.

[11] T. G. Petheram, P. G. Hourigan, I. M. Emran, and C. R. Weatherley, "Dropped head syndrome: A case series and literature review," *Spine*, vol. 33, no. 1, pp. 47–51, 2008.

[12] J. P. Drain, S. S. Virk, N. Jain, and E. Yu, "Dropped head syndrome: A systematic review," *Clin. Spine Surg.*, vol. 32, no. 10, pp. 423–429, 2019.

[13] V. Askins and F. J. Eismont, "Efficacy of five cervical orthoses in restricting cervical motion: A comparison study," *Spine*, vol. 22, no. 11, pp. 1193–1198, 1997.

[14] T. D. Kelani et al., "The influence of cervical spine angulation on symptoms associated with wearing a rigid neck collar," *Geriatr. Orthopaedic Surg. Rehabil.*, vol. 12, 2021, Art. no. 21514593211012391.

[15] K. Mekata, T. Takigawa, J. Matsubayashi, K. Toda, Y. Hasegawa, and Y. Ito, "The effect of the cervical orthosis on swallowing physiology and cervical spine motion during swallowing," *Dysphagia*, vol. 31, pp. 74–83, 2016.

[16] A. S. A. Doss, P. K. Lingampally, G. M. T. Nguyen, and D. Schilberg, "A comprehensive review of wearable assistive robotic devices used for head and neck rehabilitation," *Results Eng.*, vol. 19, 2023, Art. no. 101306.

[17] H. Zhang, B.-C. Chang, P. Kulkarni, J. Andrews, N. A. Shneider, and S. Agrawal, "Amyotrophic lateral sclerosis patients regain head-neck control using a powered neck exoskeleton," in *Proc. 9th IEEE RAS/EMBS Int. Conf. Biomed. Robot. Biomechatronics*, 2022, pp. 01–06.

[18] D. Demaree, J. Brignone, M. Bromberg, and H. Zhang, "Preliminary study on effects of neck exoskeleton structural design in patients with amyotrophic lateral sclerosis," *IEEE Trans. Neural Syst. Rehabil. Eng.*, vol. 32, pp. 1841–1850, 2024.

[19] Y. Dai, P. Shi, H. Zheng, S. Li, and F. Fang, "Design and kinematics analysis of powered cervical exoskeleton based on human biomechanics," *J. Shanghai Univ. Sci. Technol*, vol. 44, pp. 18–26, 2022.

[20] A. Lozano, M. Ballesteros, D. Cruz-Ortiz, and I. Chairez, "Active neck orthosis for musculoskeletal cervical disorders rehabilitation using a parallel mini-robotic device," *Control Eng. Pract.*, vol. 128, 2022, Art. no. 105312.

[21] P. K. Lingampally and A. A. Selvakumar, "Kinematic and workspace analysis of a parallel rehabilitation device for head-neck injured patients," *FME Trans.*, vol. 47, no. 3, pp. 405–411, 2019.

[22] H. Zhang and S. K. Agrawal, "Kinematic design of a dynamic brace for measurement of head/neck motion," *IEEE Robot. Automat. Lett.*, vol. 2, no. 3, pp. 1428–1435, Jul. 2017.

[23] M. Xiloyannis et al., "Soft robotic suits: State of the art, core technologies, and open challenges," *IEEE Trans. Robot.*, vol. 38, no. 3, pp. 1343–1362, Jun. 2022.

[24] C. M. Harbauer, M. Fleischer, T. Nguyen, F. Bos, and K. Bengler, "Too close to comfort? a new approach of designing a soft cable-driven exoskeleton for lifting tasks under ergonomic aspects," in *Proc. 2020 IEEE 3rd Int. Conf. Intell. Robotic Control Eng.*, 2020, pp. 105–109.

[25] A. T. Asbeck, R. J. Dyer, A. F. Larusson, and C. J. Walsh, "Biologically-inspired soft exosuit," in *Proc. 2013 IEEE 13th Int. Conf. Rehabil. Robot.*, 2013, pp. 1–8.

[26] M. Holewun and W. Lotens, "The influence of backpack design on physical performance," *Ergonomics*, vol. 35, no. 2, pp. 149–157, 1992.

[27] M. Xiloyannis, D. Chiaradia, A. Frisoli, and L. Masia, "Physiological and kinematic effects of a soft exosuit on arm movements," *J. Neuroengineering Rehabil.*, vol. 16, pp. 1–15, 2019.

[28] I. Bales and H. Zhang, "A six degrees-of-freedom cable-driven robotic platform for head–neck movement," *Sci. Rep.*, vol. 14, no. 1, 2024, Art. no. 8750.

[29] M. Shoaib, C. Y. Lai, and A. Bab-Hadiashar, "A novel design of cable-driven neck rehabilitation robot (carNeck)," in *Proc. IEEE/ASME Int. Conf. Adv. Intell. Mechatron.*, 2019, pp. 819–825.

[30] J. D. Mortensen, A. N. Vasavada, and A. S. Merryweather, "The inclusion of hyoid muscles improve moment generating capacity and dynamic simulations in musculoskeletal models of the head and neck," *PLoS One*, vol. 13, no. 6, 2018, Art. no. e0199912.

[31] X. Jin, X. Cui, and S. K. Agrawal, "Design of a cable-driven active leg exoskeleton (C-ALEX) and gait training experiments with human subjects," in *Proc. 2015 IEEE Int. Conf. Robot. Automat.*, 2015, pp. 5578–5583.

[32] N. Yoganandan, F. A. Pintar, J. Zhang, and J. L. Baisden, "Physical properties of the human head: Mass, center of gravity and moment of inertia," *J. Biomech.*, vol. 42, no. 9, pp. 1177–1192, 2009.

[33] V. F. Ferrario, C. Sforza, G. Serrao, G. Grassi, and E. Mossi, "Active range of motion of the head and cervical spine: A three-dimensional investigation in healthy young adults," *J. Orthopaedic Res.*, vol. 20, no. 1, pp. 122–129, 2002.

[34] D. Demaree and H. Zhang, "A structurally enhanced neck exoskeleton to assist with head-neck motion," in *Proc. 2023 IEEE Int. Symp. Med. Robot.*, 2023, pp. 1–7.

[35] H. Zhang, B.-C. Chang, Y.-J. Rue, and S. K. Agrawal, "Using the motion of the head-neck as a joystick for orientation control," *IEEE Trans. Neural Syst. Rehabil. Eng.*, vol. 27, no. 2, pp. 236–243, Feb. 2019.

[36] D. H. Gates, L. S. Walters, J. Cowley, J. M. Wilken, and L. Resnik, "Range of motion requirements for upper-limb activities of daily living," *Amer. J. Occup. Ther.*, vol. 70, no. 1, pp. 7001350010p1–7001350010p10, 2016.

[37] A. Prado, H. Zhang, and S. K. Agrawal, "Artificial neural networks to solve forward kinematics of a wearable parallel robot with semi-rigid links," in *Proc. 2021 IEEE Int. Conf. Robot. Automat.*, 2021, pp. 14524–14530.